Noise from Flight Procedure Designed with Statistical Wind: Auralization and Psychoacoustic Evaluation

Noise from Flight Procedure Designed with Statistical Wind: Auralization and Psychoacoustic Evaluation

Evangelia Maria Thoma *
Chalmers University of Technology, Gothenburg, Sweden, 412 96

Roberto Merino-Martínez †
Delft University of Technology, Delft, the Netherlands, 2629 HS

Tomas Grönstedt ‡ and Xin Zhao §
Chalmers University of Technology, Gothenburg, Sweden, 412 96

Optimal procedure design through high-precision navigation is one of the most effective ways towards sustainable aviation. By re-designing approach procedures, it is possible to reduce the noise exposure on the ground and minimize the amount of population negatively affected by it in the near-airport areas. In this study, an optimal Required Navigation Performance Authorisation Required (RNP AR) approach procedure designed using statistical historical wind data for minimum noise impact is presented. An analytic comparison of the existing and designed RNP AR procedure around Landvetter Airport in Gothenburg (Sweden) is performed in terms of sound exposure level contours, amount of affected population, auralization, and psychoacoustic sound quality metrics. It is demonstrated that, by re-constructing the lateral profile and allowing the aircraft to turn near the runway, a significant reduction of over $1/3$ in the number of people initially affected by noise exceeding 70 dB(A) in terms of sound exposure level can be achieved. However, this comes at the expense of shifting the noise contour towards urban areas that were not previously affected. Auralization and perception-based analyses are used to evaluate the perceived annoyance by the people in the near-airport area, and it is shown that a relatively small reduction in overall psychoacoustic annoyance can be achieved by the new procedure.

I. Introduction

The areas in proximity to airports are usually most affected by noise and emissions from landing and departing aircraft. Aircraft trajectory optimisation and procedure design have been commonly used as a practice for reducing the environmental impact of aircraft. However, once aircraft enter the Terminal Maneuvering Area (TMA), the allowed procedural changes are usually limited and, in most airports, aircraft must follow pre-designed procedures both for departure and approach. These procedures are designed based on the regulations set by the International Civil Aviation Organization (ICAO) in Doc 8168 [1, 2] and Doc 9905 [3]. According to these regulations, when designing non-straight flight procedures, there are two options regarding the calculation of the turn radius; (1) assuming standardized meteorological conditions with regard to wind (ICAO standard wind) and temperature, or, (2) applying historical meteorological data from the procedure location (statistical wind) if the source and values used are well documented. Flight procedure design has commonly been made using the former approach. However, following the second approach could potentially result in more efficient procedures with enhanced noise and fuel-saving benefits.

Most studies related to procedure design in the TMA focus on optimization and automatic design of departure and arrival procedures for single path [4–9] or for multiple routes and high traffic management [10–12]. Through these proposed methodologies, it is possible to control to some extent the noise levels on the ground and they can be very useful as decision-support tools when designing new procedures. However, the designed procedures cannot be implemented directly, as they must be assessed and approved first. Only a limited number of studies can be found for procedure design following the ICAO regulations. Behrend and De Smedt [13], followed the design process suggested

*Ph.D. Candidate, Fluid Dynamics Division, Department of Mechanics and Maritime Sciences, marily@chalmers.se
†Assistant Professor, Aircraft Noise & Climate Effects section, Faculty of Aerospace Engineering, r.merinomartinez@tudelft.nl
‡Full Professor, Fluid Dynamics Division, Department of Mechanics and Maritime Sciences
§Researcher, Fluid Dynamics Division, Department of Mechanics and Maritime Sciences

in ICAO Doc 8168 with standard wind conditions to explore the possibility of using the Radius-to-Fix (RF) leg in higher altitudes and for departure procedures, as well as enhancing TMA operations by integrating the usage of Global Navigation Satellite System (GNSS) for vertical navigation. The latter, referred to in their study as Enhanced Terminal Area, is used for designing efficient curved operations where the turn is performed close to the runway resulting in improved fuel consumption and reduced noise impact. Although this statement is generally true as aircraft avoid flying over inhabited areas, no detailed assessment of the potential noise benefits was provided in their study. A study that is closely related to the present work, because it incorporates the use of historical meteorological data, was performed within the project Validation and Improvement of Next Generation Airspace (VINGA) [14]. Within this project, a preliminary study of assessing curved flight procedures with statistical wind data was performed and a significant fuel benefit, ranging from 22 to 90 kg of fuel per flight, was demonstrated [15], which shows the benefits of high-precision aircraft navigation incorporating statistical wind.

In the present work, a procedure designed in a much more detailed and practical approach than that in the VINGA project is used following the revised ICAO regulations with an updated meteorological database. A quantitative noise assessment of the designed procedure is performed to evaluate any improvements in terms of the amount of affected population and the noise annoyance caused. Noise contours over the affected areas are presented to quantify any changes while a perception-based evaluation is performed using auralization and psychoacoustic evaluation. Auralization has been a growing field within aircraft noise for the last two decades. Several studies have been published [16–19] mainly focusing on evaluating future aircraft technologies. In this study, it is shown that it can also be used to facilitate the decision-making process when it comes to procedure design.

The methodologies used in the present study are described in Sec. II, starting with an overview of the procedure design, followed by the introduction of the aircraft and engine performance and noise prediction models, and a description of the auralization procedure and the computation of the psychoacoustic sound quality metrics. In Sec. III, the noise impact of the two procedures is assessed, firstly in terms of sound exposure level contours and affected population, followed by auralization and the psychoacoustic evaluation for three selected observer locations. Finally, key findings from this analysis are summarized and discussed in Sec. IV.

II. Methodology

A. Procedure Design

As part of our previous work, on-site statistical wind data covering 10 years had been used instead of the ICAO standardized wind to design a Required Navigation Performance Authorisation Required (RNP AR) approach procedure for runway 03 in Landvetter Airport in Gothenburg, Sweden [20]. The procedure design was conducted by professional procedure designers from the owner and operator of the airport with practical design experience. The design criteria for the RF leg of the two procedures are included in Table 1. The terms GGXX1 and GGXX2 in the table represent reference points marking the beginning and end of the turn, respectively, while GGARC indicates the center of the turn. GG is used to indicate that the points refer to Landvetter Airport in Gothenburg with ICAO airport identifier ESGG.

Table 1 Design criteria for the RF leg of the RNP AR procedures. (IAS: Indicated airspeed; TWC: Tailwind component;)

	Start point	End point	Center of the turn	Radius of the turn	IAS	Bank angle	TWC
ICAO standard wind	-	GGXX2 57°37’33.78"N 012°14’46.98"E	-	1.954 NM	185 kt	25°	52.44 kt
Statistical Wind – directional basis	GGXX1 57°39’03.76"N 012°09’12.79"E 2720 ft	GGXX2 57°37’33.78"N 012°14’46.98"E 1032 ft	GGARC 57°38’17.66"N 012°11’58.87"E	1.676 NM	185 kt	25°	33.9 kt

The nominal flight path of the new procedure is illustrated in Fig. 1 with the black colored line. In the same figure, the points GGXX1 and GGXX2 from Table 1 are also indicated. The red line indicates the flight path of the comparable

RNP AR procedure designed with ICAO standard wind. It can be observed that the turn radius of the test procedure is reduced leading to the aircraft avoiding flying over the populated area of Mölnlycke, marked with the blue rectangle in Fig. 1, and, therefore, to an expected reduction in the number of people severely affected by noise from approaching aircraft. In this study, the term "severely affected" refers to people living in areas where the sound exposure level exceeds 70 dB(A).

The designed RNP AR procedure has been evaluated using an Airbus A320 full-flight simulator. During the simulator session, different cases were tested and the procedure was assessed for feasibility, crew workload, and aircraft drift. In all cases, the procedure was regarded as viable both in terms of flyability and operability.

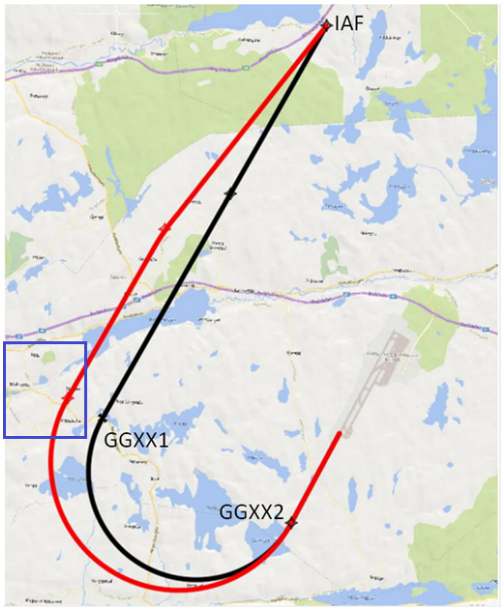

Fig. 1 Procedures designed with ICAO standard wind (red) and statistical meteorological data (black) [20].

B. Aircraft Model and Engine Performance

The aircraft and engine model development have been described and validated against official public performance data in [21]. For the engine performance estimation, the in-house code GESTPAN [22] was used. The required inputs for GESTPAN were calculated from the designed procedures and the flight dynamics model following the same process as in [23].

C. Aircraft Source Noise Prediction

The noise generated from an aircraft consists of the combination of the contributions of all the propulsive and non-propulsive (airframe) components. The relative contribution of each component depends on several factors, such as aircraft and engine technology and operational conditions. The aircraft is typically assumed to be a point source with a total noise emission equal to the sum of all these components. In this work, each component was modelled independently using empirical and semi-empirical models that are found in the public literature. The implementation has been described in detail and validated in [23] and the open-source Python Library, CHOICE, can be accessed through GitHub [24].

D. Propagation in the Atmosphere

For a moving source, the characteristics of the sound, frequency, and amplitude, vary as it reaches an observer. The frequency experiences a shift, known as the Doppler effect while the amplitude is modified through convective amplification.

As sound travels through the atmosphere, several other effects affect its characteristics before it reaches an observer on the ground. These effects include atmospheric absorption, calculated here according to the ISO 9613-1:1993

standard [25], spherical spreading, change in atmospheric characteristic impedance, and ground reflection, which in this work was modelled according to the method presented by Chien and Soroka [26].

The propagation model implemented in this work assumes a standard non-refractive atmosphere with zero wind.

E. Population Data

The population grid used in this study is from EU GHSL – Global Human Settlement Layer data [27] and is the spatial raster dataset that depicts the distribution of the residential population. Once the sound exposure level (SEL) on the ground was determined for each procedure, the population grid was interpolated to estimate the noise-affected residents, within the desired limit.

F. Noise Synthesis

Auralization of aircraft noise can be performed either by following a time-domain or a frequency-domain approach. A detailed description of these two approaches was presented by Rizzi and Sahai [17]. Both approaches should theoretically result in the same receiver pressure time history. However, because frequency-domain propagation is usually performed in one-third octave band frequencies, some phase information is lost during the propagation [17]. Thus, in the present study, a combination of both approaches was implemented according to which certain frequency-dependent propagation effects, namely atmospheric absorption and ground reflection, were applied in the time domain through filtering operations. The source noise prediction with the Doppler effect and spherical spreading were performed in the frequency domain, as described in the previous sections. Two separate synthesis procedures were then performed for the broadband and tonal noise components, respectively.

Broadband noise was estimated in one-third octave bands and was synthesized using the overlap-add method [16, 28]. The spectrum was first converted to a narrowband spectrum, according to the selected block size, and a random phase was assigned to each frequency component. An Inverse Fast Fourier Transform (IFFT) was then applied to obtain the pressure time history. This process was repeated for every time step. The time between consecutive time steps, namely the hop size, was selected to be smaller than the block size. This way, the blocks overlapped with each other resulting in a smooth transition between consecutive time steps. Each block was then multiplied by a Hanning window and added to the previous block, ensuring the correct acoustic energy values. In the present study, the synthesis was performed at a sampling rate of 44.1 kHz with a hop size of 512 samples (or 11.6 ms) and a block size of 8192 samples (or 185.6 ms).

The tonal noise synthesis was performed using an additive synthesis technique where the pressure time history of each tone is modelled as a cosine wave [16, 28]. For each engine tonal noise source, the Doppler-shifted blade-passing-frequency (BPF) and its harmonics were used to determine the frequency and amplitude of the harmonics in the predicted one-third octave band spectra at each aircraft state [29], which corresponded to the beginning of a synthesis block. Interpolation was used to ensure a smooth transition between aircraft states. Care was taken so that the phase at the end of a synthesis block, matched the one at the beginning of the next. This smooth transition ensured that audible artifacts were avoided.

Atmospheric absorption and ground reflection were modelled in the frequency domain according to the methods described in Sec. II.D. The resulting spectra were converted to finite impulse response (FIR) filters through an IFFT. The impulse response was shifted by $N_s/2$ samples and truncated to the desired number of N_s filter taps resulting in a linear phase filter. The application of the filters was performed through convolution, after which the first $N_s/2$ samples were discarded to account for the delay caused by the linear phase filter [30–32]. The ground reflection model was further enhanced by including a turbulence-induced coherence loss factor as described by Arntzen [28].

When the purpose of the auralization is to assess one or more flight procedures, as in the present study, it is highly unlikely that during these procedures there are no changes in configuration or operating conditions. In reality, these changes are gradual, but in simulations, they occur instantaneously, resulting in discontinuities in performance parameters and noise levels. This is usually not an issue when noise impact is assessed through noise mapping using time-averaged sound metrics but it will cause audible artifacts in auralizations. For this reason, flight performance data were smoothed in the design process, while changes in configuration were simulated by linearly interpolating the mean square acoustic pressure over a time span of 10 s for the slat extension to configuration 1 and for the landing gear deployment and 5 s for the flap extension and for the rest of the slat positions. These values were approximated from available flight data.

A comparison of a synthesized sound, from available flyover data, with the corresponding noise measurement data is presented in the spectrograms in Fig. 2, for an approach procedure performed by an A321neo with LEAP-1A engine. The available flyover data and measurements were gathered as part of the ANT (Approach Noise Trials) project [33]

during which consecutive approach flights were performed over a series of microphones placed along the ground track of the approach path on runway 26 at Arlanda airport in Stockholm. The experimental campaign was described by Åbom *et al.* [33] and Johansson [34]. The data used for the validation in this study correspond to a microphone, with a height of 1.6 m, located 4.7 nm from the runway threshold. The location of this microphone can be found in Figure 2 of the corresponding report [33], indicated as Mic 4.7nm. During the specific flyover the average atmospheric temperature was -1.8 $^{\circ}C$ and the average wind speed recorded by the flight recorder was 5 m/s with direction from the west and northwest. The terrain of the measurement site was mainly flat and consisted primarily of agricultural landscapes.

For this case only, the synthesis was performed with a sampling frequency of 48 kHz with a block time step of 0.125 s to match the settings used in the measured experimental data. During the indicated time, the aircraft configuration was set to 2, i.e. slats deployed at 22° and flaps at 14°, while the landing gear deployment started at 00 : 00 : 00 (see horizontal axes in Fig. 2). The SEL value predicted by the synthesis amounted to 79.8 dB(A) with a maximum A-weighted sound pressure level of 70.9 dB(A), whereas the recorded sound was estimated at 78.9 dB(A) with a maximum of 70.2 dB(A). In the two spectrograms, an overall good agreement can be observed but a few differences can be noted. The shapes of the two spectrograms match well, although, the synthesis indicates a slightly higher low-frequency content than the recording. This increased low-frequency contribution can be attributed to the implemented landing gear noise prediction model, which suggests an increase in frequencies below 300 Hz [23], while this frequency region is also less affected by the atmospheric attenuation effect. Another noticeable difference is caused by the background noise in the recording (songbird, vegetation motion from the wind, etc.) which appears as high-frequency noise before and after the peak in the flyover aircraft noise. In the recorded spectrogram, some vertical lines can also be observed, which correspond to temporal variations at the source and atmospheric turbulence affecting the propagation [28, 29, 31, 35]. These are not present in the synthesized cases, which are based on the time-averaged models employed, which do not include short-term variations or atmospheric turbulence effects. Finally, although not very distinct, some differences in the tonal noise components can be observed. In the synthesis, two variable tones can be observed, which are related to the harmonics of the BPF. These tones are slightly overpredicted, which could be attributed to the simple noise suppression model. In the experimental recording, two different tones can be seen at about 700 Hz in the beginning and at 1600 Hz at the end of the spectrogram, which are not visible in the synthesized case. After examination of these tones, it was concluded that they are probably caused by cavities in the nose landing gear (higher-frequency tone) [36–38] and possibly the fuel vent opening on the wing (lower frequency tone) [37, 39]. These tones are difficult to predict accurately, especially with semi-empirical models, such as the ones used in the present study.

When listening to the auralized and recorded audio files, which can be found on the Research website of Chalmers University of Technology [40], similar observations can be made. The most distinct difference comes from the binaural effect of the recording which is not currently included in the auralization. The amplitude modulations caused by the atmospheric turbulence are also evident in the recording, while the difference in tonal components can also be noticed. Overall, despite the observed differences, which are mainly attributed to the limitations of the semi-empirical noise models and create a somewhat more artificial sensation, it is believed that the tool can capture the main characteristics of the sound and can be used for the relative assessment of different sound scenarios.

G. Psychoacoustic Evaluation

Sound Quality Metrics (SQMs) describe the subjective perception of sound by human hearing, unlike the sound pressure level metric, which quantifies the purely physical magnitude of sound based on the pressure. Previous studies [41, 42] showed that these metrics better capture the auditory behavior of the human ear compared to conventional sound metrics typically employed in noise assessments. The five most commonly-used SQMs [43] are:

- Loudness (N): Subjective perception of sound magnitude corresponding to the overall sound intensity [44].
- Tonality (K): Measurement of the perceived strength of unmasked tonal energy within a complex sound [45].
- Sharpness (S): Representation of the high-frequency sound content [46].
- Roughness (R): Hearing sensation caused by sounds with modulation frequencies between 15 Hz and 300 Hz [47].
- Fluctuation strength (FS): Assessment of slow fluctuations in loudness with modulation frequencies up to 20 Hz, with maximum sensitivity for modulation frequencies around 4 Hz [48].

These five SQMs were then combined into a single global psychoacoustic annoyance (PA) metric following the model outlined by Di *et al.* [49].

All the SQMs and the PA metric were computed using the open-source MATLAB toolbox SQAT (Sound Quality Analysis Toolbox) v1.0 [43, 50]. The GitHub repository of the toolbox can be found in [51].

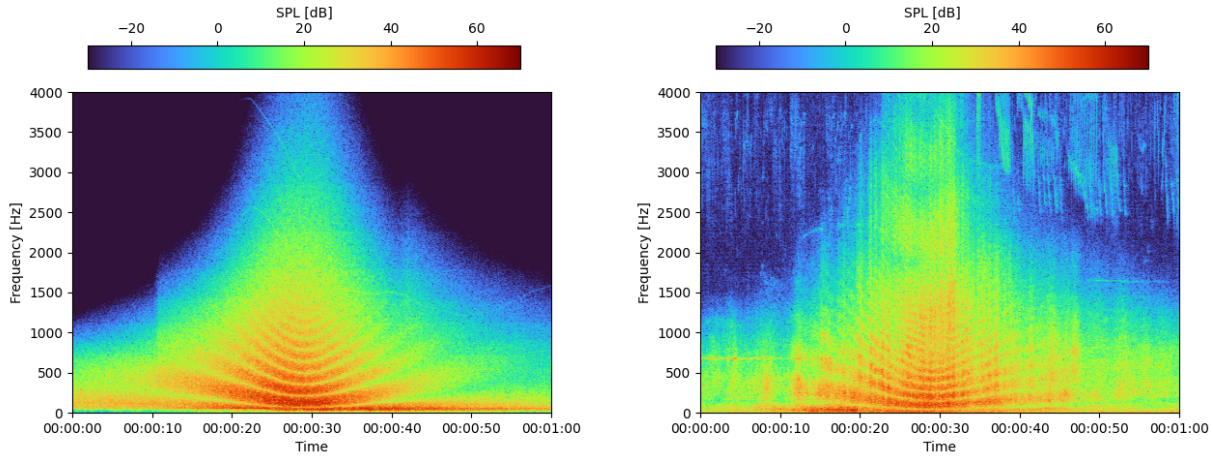

(a) Synthesized **(b) Measured**

Fig. 2 Spectrograms of the synthesized (a) and measured (b) aircraft (A321neo with LEAP-1A engine) flyover noise.

III. Results

The flight profile and power requirement for the two procedures are presented in Fig. 3. In both cases, the initial altitude and speed of the aircraft are the same, marking the entry point to the initial approach segment. As the procedure with statistical wind data is shorter, the aircraft needs to descend faster, therefore, a higher descent angle is observed in the first part of the descent, resulting in a slightly lower power requirement. The aircraft velocity is maintained constant until the 20 km mark is reached and the deceleration starts. When the aircraft reaches the final approach point (FAP), the same velocity is used in both cases and the slats have been extended (configuration 1). After this point, configuration 2 is set and a normal approach is performed, i.e. descent with a 3° flight path angle. In both cases, the extension of the slats results in a sudden decrease in thrust, which is caused by the sudden increase in drag. The landing gear is deployed at an altitude of 1900 ft or 579 m followed by configuration 3. As can be observed, the profiles of the two procedures are very similar, especially after the aircraft reaches a distance of 10 km from the threshold, since the purpose of this study was to evaluate the two procedures when flown in a similar manner and under the same conditions.

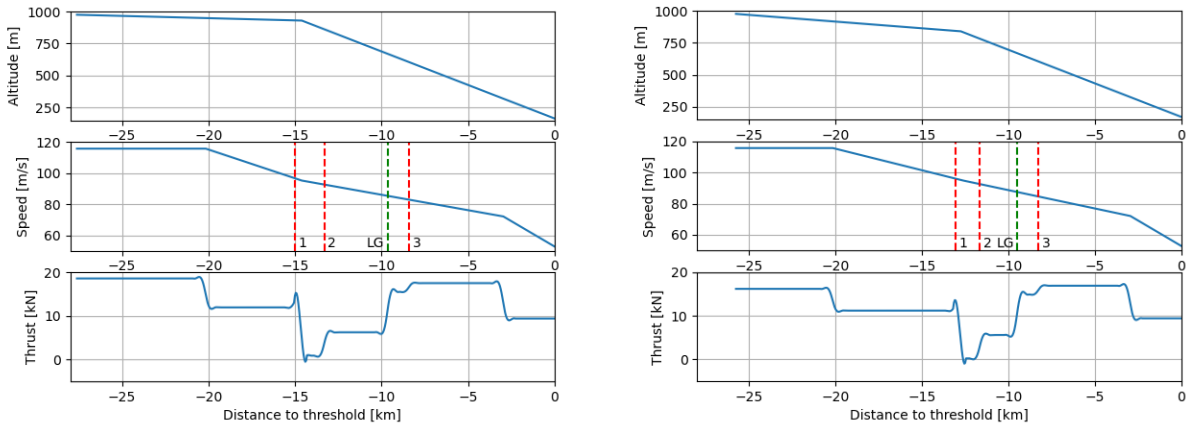

(a) Standard wind **(b) Statistical wind**

Fig. 3 Flight profile for the procedure designed with (a) ICAO standard wind and (b) statistical meteorological data. The vertical lines indicate the configuration changes and LG denotes the landing gear deployment.

The SEL contours for the two procedures are shown in Fig. 4. This metric represents the cumulative sound energy of an occurrence, taking into consideration both the A-weighted noise level experienced and the duration of exposure. It is, therefore, a good metric for comparing aircraft noise events with different durations. In Fig. 4, the location of the configuration changes is also indicated in terms of slat and flap angles and landing gear position. It can be observed that the total contour area is reduced in the case of the test procedure (designed using statistical meteorological data) as the total path length and turn radius have been reduced. The isolines of the contours have, generally, been displaced towards the right, and although areas such as Lindome (light blue rectangle in Fig. 4) and Öjersjö (orange rectangle in Fig. 4) are experiencing less noise, the areas located on the inside of the turn are more affected from the new procedure. As the turn radius has been decreased, the aircraft flies close to these areas for a longer time, resulting in increased noise exposure.

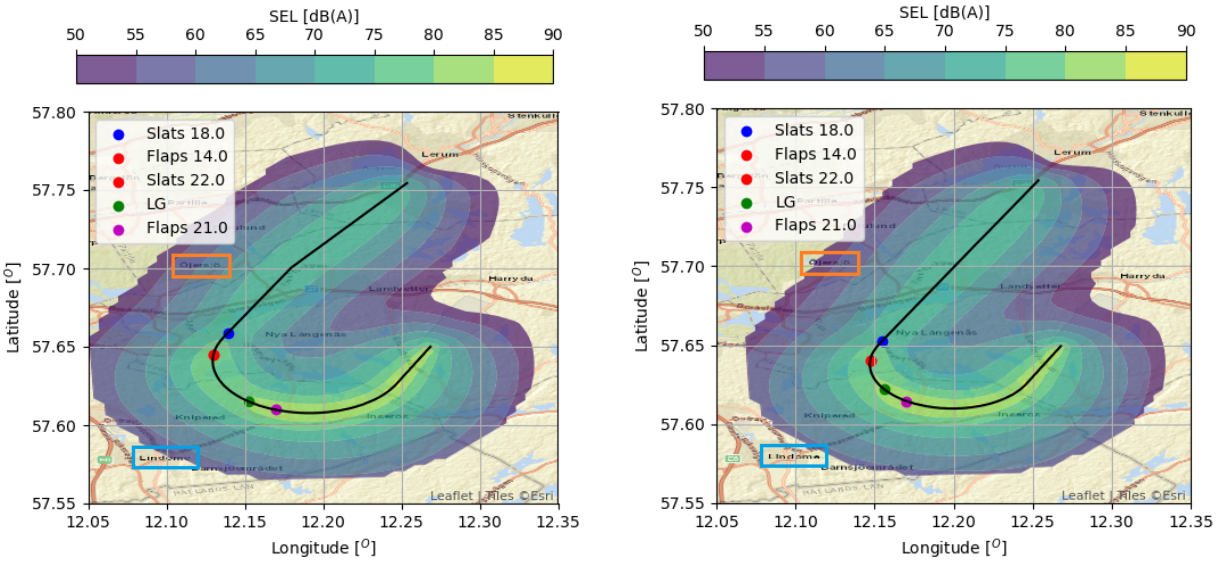

(a) Standard wind **(b) Statistical wind**

Fig. 4 SEL contours for the procedure designed with (a) ICAO standard wind (b) and statistical meteorological data.

In order to better quantify the effect on the local population, Fig. 5 shows the affected population from each of the two procedures. The red and black symbols correspond to the number of people living in an area where the SEL exceeds 70 dB(A) for the existing and the test procedures, respectively. More specifically, the affected population, initially amounting to 15506 people with the standard wind procedure, was reduced by about 5760 people, indicating that the noise contours have shifted towards less densely populated areas.

At this point, it is interesting to note that even though the number of affected people decreased, redesigning the flight path results in a relocation of the noise-affected areas meaning that the number of people who were experiencing noise annoyance before will be reduced, but also that people who were not affected before will now be affected by the new procedure. It, therefore, comes down to an ethical dilemma; *should the existing procedure be kept with no effect on the noise-affected population, or should the new procedure be implemented, reducing the total number of affected people but causing annoyance for people who were less severely affected before?*

Questions like this are usually the responsibility of the decision-makers to answer. However, it is important to not only look at the number of people but also to evaluate the noise impact and annoyance in more detail. Although SEL contours are an important and necessary tool for evaluating the noise impact around airports, they do not provide much information on the human perception of the noise and the annoyance experienced by people. It is, therefore, necessary to include tools in the decision-making process that will help in understanding people's reactions to new procedures. Such tools are for example auralization and psychoacoustic evaluation. For this purpose, three representative points were selected to perform a more detailed analysis of the noise impact. These points are indicated in Fig. 5 with circles of a different colour (purple, green, and blue), and labeled as "P1", "P2" and "P3", respectively. The locations were chosen with careful consideration: one to represent the population predominantly influenced by the new procedure (P1), another to reflect the population primarily affected by the standard wind procedure (P3), and a third location where

the population experiences effects in both cases (P2). The latter was chosen to assess whether the perceived noise annoyance has changed. The coordinates of the selected observer locations, as well as the minimum source-observer distance for each case, are presented in Table 2. The locations represented by P2 and P3 correspond to preschools also surrounded by playgrounds and parks. P1 is located in a smaller community without any schools and, thus, the center of the community was chosen as the focal point.

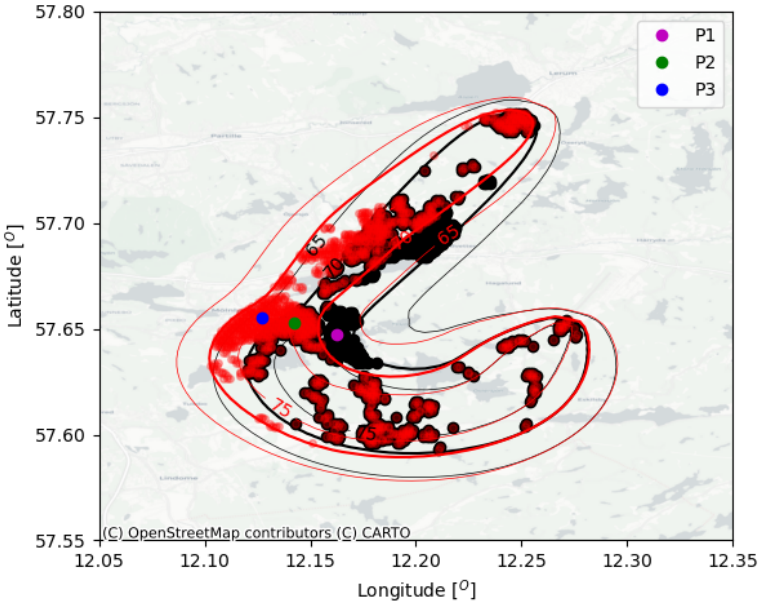

Fig. 5 SEL contour lines and population exposed to noise level higher than 70 dB(A) depicted as dots for the standard (red) and test procedure (black).

Table 2 Geographical coordinates and minimum source-observer distances for the selected observer locations.

	Coordinates, [°]		Minimum distance, [m]	
Point	Latitude	Longitude	Standard	Statistical
P1	57.6475	12.1624	1980	998
P2	57.6526	12.1425	970	992
P3	57.6551	12.1270	961	1768

The spectrograms for the synthesized flyovers are presented in Fig. 6 for the three selected observer points and the two procedures. The results are presented from the rightmost to the leftmost point, i.e. P1 to P3, in Fig. 5. Thus, Fig. 6a and Fig. 6b correspond to P1 in Fig. 5, whereas, Fig. 6e and Fig. 6f correspond to P3. The spectrograms are presented only for the time when the aircraft is closest to the respective selected points, marked with dashed black lines in Fig. 6, and the $L_{A,max}$ value is reached. The indicated time is calculated relative to the start of the procedure from the initial approach segment (t = 0 s). For the standard procedure, the indicated time period corresponds to the segment between, approximately, 17.3 km and 11.6 km from the runway threshold and, for the test procedure, between 15.6 km and 9.9 km. In both cases, this segment includes two configuration changes, i.e. extension of slats to configuration 1 and extension of flaps and further extension of slats to configuration 2.

As the aircraft performance is similar in both procedures, there are no major differences observed at the component level. Two tonal components can be observed in all cases, one starting at a frequency between 3500 kHz and 4000 kHz, and one less pronounced starting at around 2000 kHz. These correspond to fan tones occurring at harmonics of the BPF, and, as was expected from Fig. 3, the tonal frequencies for the standard procedure are slightly higher compared

to the new procedure, due to the higher power requirement. The gradual decrease in tonal frequency is due to the Doppler effect, as the aircraft moves closer to the selected observer location, while the tones disappear almost completely once the slats are fully deployed at 18° and the thrust drops to idle, see Fig. 3. An increase in noise levels can be noticed between 00 : 01 : 50 and 00 : 02 : 00, which is driven by the increase in aerodynamic noise as the slats are gradually extended. This is somewhat counterbalanced when the thrust decreases. The noise increment when flaps are deployed and slats are further extended to configuration 2 is smaller and, thus, it is not as noticeable in the spectrograms. Perhaps one of the most prominent differences between the spectrograms from each procedure for a specific point is the interference pattern from the ground reflection effect. In Fig. 6a the distance between source and observer is larger than in Fig. 6b resulting in a less pronounced interference pattern and reduced noise level. Similarly, the source-observer distance in Fig. 6e is smaller than in Fig. 6f. For P2, the distance and, hence, the interference pattern between direct and reflected sound ray path, is similar for both procedures. As was also observed from Fig. 4, it becomes evident from the spectrograms that the noise in P1 increases when the test procedure is used, while a reduction in P3 can be observed. With regard to P2, a small improvement can be noticed when using the new procedure. For further evaluation, a more subjective assessment of the perceived noise would provide a more valuable insight.

The duration of the corresponding synthesized sound files [40] is 20 seconds, with a starting time 10 seconds before the $L_{\mathrm{A,max}}$ value is reached, which varies from 00 : 01 : 57 for the case in Fig. 6e to 00 : 02 : 02 for the case in Fig. 6f. When listening to the synthesized audio files, it makes sense to compare P1 from the standard wind procedure with P3 from the statistical wind procedure and, similarly, P3 from the standard procedure with P1 from the statistical. This way, it is possible to evaluate whether the people severely affected by the new procedure are experiencing higher or lower annoyance than the previously highly affected population. Starting with the former case, i.e. standard wind P1 and statistical wind P3, shown in Fig. 6a and Fig. 6f, respectively, the noise in the two points sounds very similar, from a first comparison, although, if one listens carefully, the noise in P3 sounds slightly louder, according to the authors' opinion. However, it is unlikely that this difference would be noticed, especially since this is the case where the lowest noise level is observed. When looking at P3 from the standard procedure and P1 from the new procedure, Fig. 6e and Fig. 6b, correspondingly, no obvious differences can be noticed in this case either, although the sound in P3 from the standard procedure seems louder. For P2, Fig. 6c and Fig. 6d, it seems that there is a small noise reduction obtained by the new procedure, which could be partly attributed to the slightly reduced thrust. The difference in the source-observer distance also has a small effect in all cases, resulting in an increase of approximately 1.0 dB for the first case, standard wind P1 and statistical wind P3, and a reduction of 0.3 dB and 0.2 dB for the second, standard wind P3 and statistical wind P1, and third case, P2, respectively. With regard to the tonal component, unless the sound files are heard consecutively, the difference in tonal frequency is not noticeable. Overall, albeit small, an improvement is achieved with the new procedure, although, evidently, the noise annoyance for the residents in P1 increases considerably. This can also be observed from the effective perceived noise level (EPNL) and $L_{\mathrm{A,max}}$ values presented in Table 3. The values in this table are in line with the observations made from the recordings and it can further be noticed that, with the new procedure, the highest noise levels are observed in P2, with a small reduction with respect to the standard procedure.

Table 3 Effective perceived noise level (EPNL) and maximum A-weighted sound pressure level ($L_{A,max}$) for the three selected points and two procedures considered.

	EPNL, [EPNdB]		$L_{A,max}$, [dB(A)]	
Case	Standard	Statistical	Standard	Statistical
P1	63.31	73.59	52.93	61.60
P2	74.37	73.00	62.78	62.19
P3	75.07	65.31	63.04	54.71

Using the synthesized sound files, the psychoacoustic sound quality metrics presented in Sec. II.G were calculated for each selected observer point and procedure. Their top 5% percentile values are presented in Fig. 7, representing the value of each metric that was exceeded for 5% of the total time history considered. As expected, the maximum loudness (N_5) is reached at P3 and closely followed by P2, when the aircraft follows the standard procedure, whereas the general loudness trend follows that of the $L_{A,max}$ metric in Table 3. Interestingly, in terms of tonality, higher values are observed for the new procedure, indicating no improvement for P3, despite the overall noise reduction. This could be explained by the higher relative prominence of the engine tonal noise in the statistical wind case since the broadband noise levels are lower. The change in sharpness seems to follow the same pattern as the metrics in Table 3, which

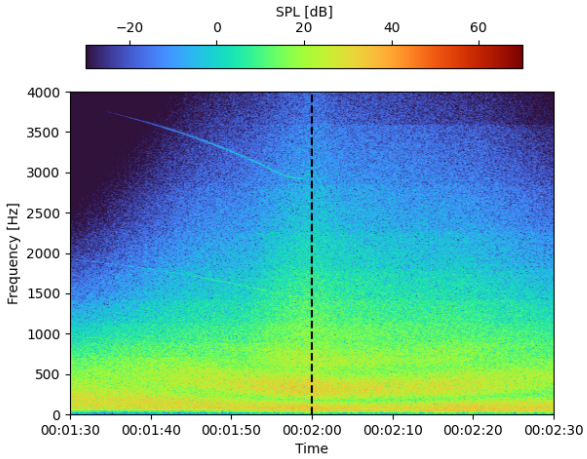

(a) P1 (purple): Standard wind

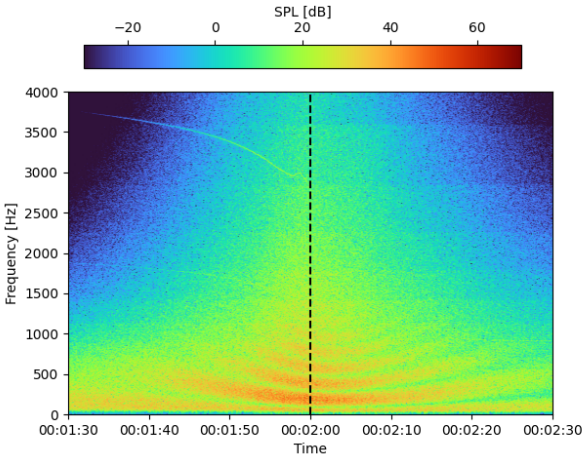

(b) P1 (purple): Statistical wind

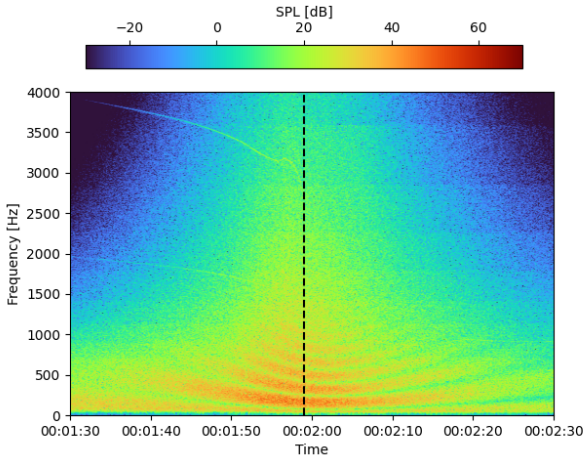

(c) P2 (green): Standard wind

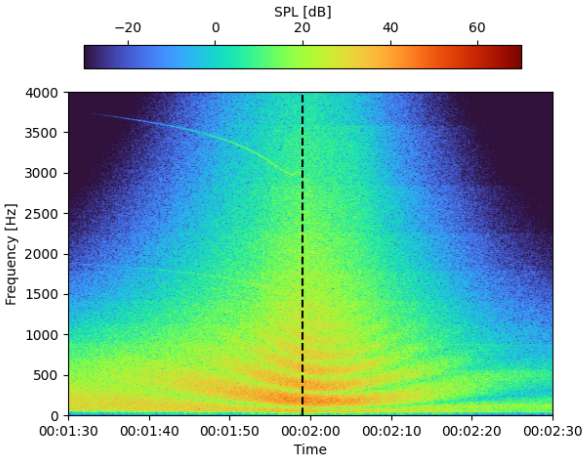

(d) P2 (green): Statistical wind

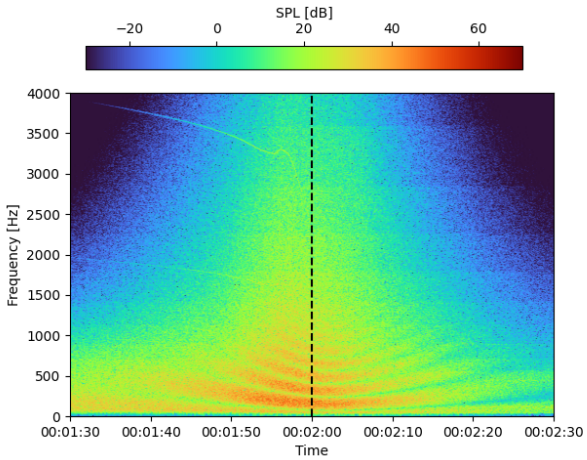

(e) P3 (blue): Standard wind

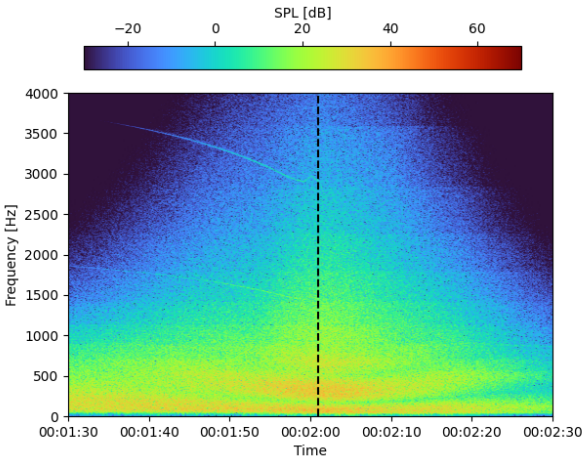

(f) P3 (blue): Statistical wind

Fig. 6 Spectrograms of the synthesized flyovers at the three selected observer points.

was expected since in all cases the signal power is more concentrated towards the lower frequencies, with a notable reduction in the high-frequency content for P1 and P3, for the standard and the statistical wind procedure, respectively.

In all cases, both the roughness and fluctuation strength metrics remain at relatively low values. The roughness from the standard procedure surpasses all the statistical wind cases, which remain almost unchanged. The low levels of fluctuation strength were expected as the source noise prediction is based on time-averaged models that do not include short-term variations and amplitude modulations caused by atmospheric turbulence were also not modelled. Finally, the global psychoacoustic annoyance metric indicates that for both procedures the annoyance for the two most affected points, i.e. P2 and P3 for the standard case and P1 and P2 for the statistical wind procedure, is almost unchanged, while a slightly lower annoyance level is observed for the two points most affected by the new procedure compared to the points affected by the standard procedure.

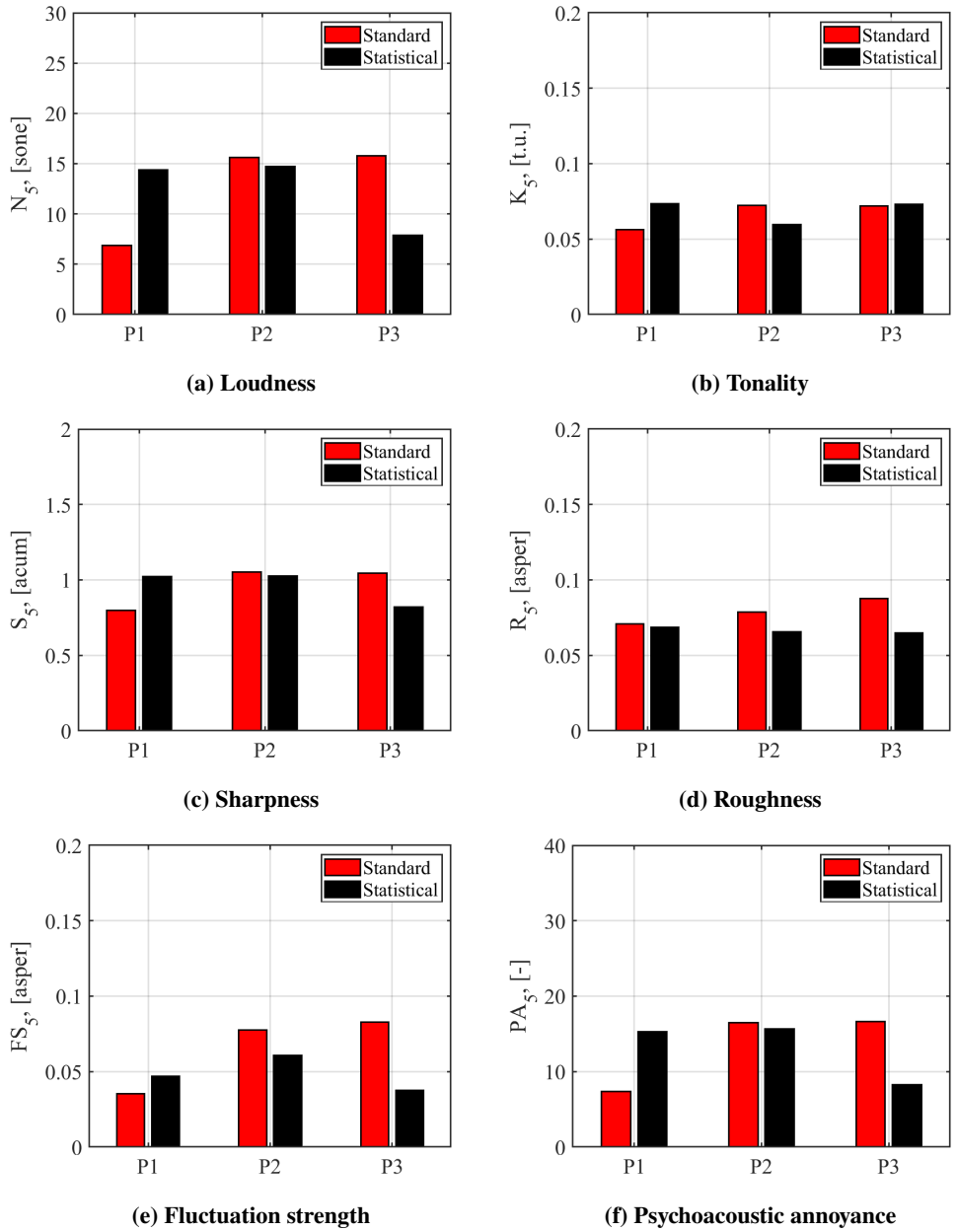

(a) Loudness **(b) Tonality**

(c) Sharpness **(d) Roughness**

(e) Fluctuation strength **(f) Psychoacoustic annoyance**

Fig. 7 Sound quality metrics for the three selected points and two procedures considered.

IV. Discussion and conclusions

In this work, the noise impact from two RNP AR approach procedures on the local communities around Landvetter Airport in Gothenburg (Sweden) has been examined. The two procedures differed in their design approach, as one followed the more commonly used design methodology, where standard ICAO wind is assumed, and the other was designed with the help of statistical meteorological data. To obtain a fair comparison, it was assumed that the procedures were flown in a similar way, i.e. that similar velocity profiles were used and that configuration changes occurred at approximately the same altitude or velocity.

The noise assessment involved a combination of prediction approaches, starting with the more conventional SEL contours which were used to determine the amount of highly affected population. This indicated that, with the new procedure, a reduction by more than $1/3$ of the initially affected population can be achieved, while the total affected area is reduced. However, as the lateral path of the procedure was shifted, with the decrease in aircraft turn radius, the highly affected areas were also displaced, resulting in increased annoyance for people who were less severely affected before. Therefore, the problem became more than just a simple question of reducing the number of highly affected people.

Auralization was used in an effort to determine whether the new procedure would result in a lower noise annoyance level. The auralizations, that were performed for three selected observer points and the two procedures, indicated a minor difference in the audible noise level when comparing the most severely affected locations from the two procedures, with the new procedure showing a slightly lower level. However, this corresponded to a notable increase in noise annoyance for the residents of the selected P1. The calculation of the psychoacoustic metrics, further supported these observations, suggesting that the standard procedure would, generally, be perceived as slightly more annoying, with only the tonality metric reaching higher values for the new statistically-based procedure.

It was not within the aim of this work to make a suggestion as to which procedure should be standardized, but merely to provide a more comprehensive analysis of the noise impact from the two cases and to show how auralization and psychoacoustic evaluation can be used to facilitate the decision-making process in procedure design. The findings indicate a significant reduction in the number of highly affected inhabitants, with the newly affected people experiencing less annoyance (although by a small amount) than the previously highly affected areas. These findings can be used by decision-makers and procedure designers to select the optimal scenario. For an even more complete view of the problem, the noise impact when the procedures are flown in different operational and weather conditions should also be examined. Finally, a more detailed evaluation could be performed by generating psychoacoustic annoyance contour maps to assess the overall noise annoyance in the area, rather than in individual selected points, while listening experiments could be performed to obtain a more representative subjective assessment of the annoyance level. The latter is already planned to take place in the near future.

Acknowledgments

The authors gratefully acknowledge the Swedish Transport Administration, Trafikverket, for funding and supporting this work through the NEFAT (TRV 2022/106392) project. The authors would also like to thank the CIDER project for the noise prediction, STATMET for the procedure design, and ANT for providing the recordings and data used for validation. The research work of Roberto Merino-Martinez belongs to the project *Listen to the future* (with project number 20247) of the research programme Veni 2022 (Domain Applied and Engineering Sciences) which is (partly) financed by the Dutch Research Council (NWO).

References

[1] "Doc 9889, Airport Air Quality Manual - Second Edition," Tech. rep., International Civil Aviation Organization (ICAO), 2020.

[2] "Doc 8168, Procedures for Air Navigation Services - Aircraft Operations Volume I - Flight Procedures - Sixth Edition," Tech. Rep. ISBN 978-92-9258-670-6, International Civil Aviation Organization (ICAO), Montréal, Quebec, Canada, 2018.

[3] "Doc 9905, Required Navigation Performance Authorization Required (RNP AR) Procedure Design Manual - Third Edition," Tech. Rep. ISBN 978-92-9265-613-3, International Civil Aviation Organization (ICAO), Montréal, Quebec, Canada, 2021.

[4] Zhou, J., Cafieri, S., Delahaye, D., and Sbihi, M., "Optimizing the Design of a Route in Terminal Maneuvering Area Using Branch and Bound," Tokyo, Japan, 2015, pp. 171–184. https://doi.org/10.1007/978-4-431-56423-2_9.

[5] Hasegawa, T., Tsuchiya, T., and Mori, R., "Optimization of Approach Trajectory Considering the Constraints Imposed on Flight Procedure Design," *Procedia Engineering*, Vol. 99, Shangai, China, 2014, pp. 259–267. https://doi.org/https://doi.org/10.1016/j.proeng.2014.12.534.

[6] Visser, H. G., and Wijnen, R. A. A., "Optimization of Noise Abatement Departure Trajectories," *Journal of Aircraft*, Vol. 38, No. 4, 2001, pp. 620–627. https://doi.org/10.2514/2.2838.

[7] Hartjes, S., and Visser, H. G., "Efficient trajectory parameterization for environmental optimization of departure flight paths using a genetic algorithm," *Proceedings of the Institution of Mechanical Engineers, Part G: Journal of Aerospace Engineering*, Vol. 231, No. 6, 2017, pp. 1115–1123. https://doi.org/10.1177/0954410016648980.

[8] Zhang, M., Filippone, A., and Bojdo, N., "Multi-objective optimisation of aircraft departure trajectories," *Aerospace Science and Technology*, Vol. 79, 2018, pp. 37–47. https://doi.org/10.1016/j.ast.2018.05.032.

[9] Zhang, M., and Filippone, A., "Optimum problems in environmental emissions of aircraft arrivals," *Aerospace Science and Technology*, Vol. 123, 2022. https://doi.org/10.1016/j.ast.2022.107502.

[10] Zhou, J., Cafieri, S., Delahaye, D., and Sbihi, M., "Optimal Design of SIDs/STARs in TMA Using Simulated Annealing," *2016 IEEE/AIAA 35th Digital Avionics Systems Conference (DASC)*, Sacramento, CA, United States, 2016, pp. 1–8. https://doi.org/10.1109/DASC.2016.7778099.

[11] Andersson Granberg, T., Polishchuk, T., Polishchuk, V., and Schmidt, C., "Automatic Design of Aircraft Arrival Routes with Limited Turning Angle," 2016, pp. 9:1–9:13. https://doi.org/10.4230/OASIcs.ATMOS.2016.9.

[12] Pfeil, D. M., "Optimization of airport terminal-area air traffic operations under uncertain weather conditions," Doctoral thesis, Massachusetts Institute of Technology, Cambridge, Massachusetts, USA, 2011. URL http://hdl.handle.net/1721.1/67716.

[13] Behrend, F., and De Smedt, D., "Simulations investigating curved departure and arrival procedures using GNSS based vertical guidance," *2018 IEEE/AIAA 37th Digital Avionics Systems Conference (DASC)*, IEEE, London, UK, 2018, pp. 1–10. https://doi.org/10.1109/DASC.2018.8569517.

[14] "SESAR Joint Undertaking | VINGA," , 2011. URL https://www.sesarju.eu/node/1538, accessed in December 2023.

[15] Wiklander, N., Cadot, E., Maier, T., Ziverts, U., Linnér, A., Eklund, R., Ekstrand, H., Hilmersson, A., and Mitchell, D., "SESAR joint undertaking - the VINGA project final report," Tech. rep., 2011.

[16] Rizzi, S. A., Aumann, A. R., Lopes, L. V., and Burley, C. L., "Auralization of Hybrid Wing–Body Aircraft Flyover Noise from System Noise Predictions," *Journal of Aircraft*, Vol. 51, No. 6, 2014, pp. 1–19. https://doi.org/10.2514/1.C032572.

[17] Rizzi, S. A., and Sahai, A. K., "Auralization of air vehicle noise for community noise assessment," *CEAS Aeronautical Journal*, Vol. 10, 2019, pp. 313–334. https://doi.org/10.1007/s13272-019-00373-6.

[18] Pieren, R., Bertsch, L., Lauper, D., and Schäffer, B., "Future Low-Noise Aircraft Technologies and Procedures - Perception-based Evaluation Using Auralised Flyovers," *Proceedings of the 23rd International Congress on Acoustics*, Aachen, Germany, 2019, pp. 1–5. https://doi.org/10.18154/RWTH-CONV-238860.

[19] Pieren, R., Le Griffon, I., Bertsch, L., Heusser, A., Centracchio, F., Weintraub, D., Lavandier, C., and Schäffer, B., "Perception-based noise assessment of a future blended wing body aircraft concept using synthesized flyovers in an acoustic VR environment—The ARTEM study," *Aerospace Science and Technology*, Vol. 144, 2024, p. 108767. https://doi.org/10.1016/j.ast.2023.108767, URL https://www.sciencedirect.com/science/article/pii/S1270963823006636.

[20] Zhao, X., Grönstedt, T., Ullvetter, M., Lukic, P., Näs, A., Larsson, I., Petit, O., Wall, M., Ziverts, U., Ekstrand, H., Linner, A., Martin, R., Johansson, , Unden, P., and Olsson, E., "Report of STATMET (En databas med STATistisk METeorologisk data för procedurkonstruktion)," Tech. rep., 2023.

[21] Thoma, E. M., Grönstedt, T., and Zhao, X., "Quantifying the Environmental Design Trades for a State-of-the-Art Turbofan Engine," *Aerospace*, Vol. 7, No. 10, 2020. https://doi.org/10.3390/aerospace7100148, URL https://www.mdpi.com/2226-4310/7/10/148.

[22] Grönstedt, T., "Development of methods for analysis and optimization of complex jet engine systems," Ph.D. Thesis, Chalmers University of Technology, Gothenburg, Sweden, 2000.

[23] Thoma, E. M., Grönstedt, T., Otero, E., and Zhao, X., "Assessment of an Open-Source Aircraft Noise Prediction ModelUsing Approach Phase Measurements," *Journal of Aircraft*, 2023. https://doi.org/10.2514/1.C037332, URL https://arc.aiaa.org/doi/10.2514/1.C037332.

[24] Thoma, E. M., Zhao, X., and Grönstedt, T., "CHOICE - CHalmers nOIse CodE," , Dec. 2022. URL https://github.com/emthm/CHOICE, accessed in December 2023.

[25] ISO, "Acoustics - Attenuation of sound during propagation outdoors Part 1: Calculation of the absorption of sound by the atmosphere," Tech. Rep. ISO 9613-1:1993, International Organization of Standarizations, 1993.

[26] Chien, C. F., and Soroka, W. W., "Sound propagation along an impedance plane," *Journal of Sound and Vibration*, Vol. 43, No. 1, 1975, pp. 9–20. https://doi.org/10.1016/0022-460X(75)90200-X.

[27] "Global Human Settlement - Download - European Commission," , 2023. URL https://ghsl.jrc.ec.europa.eu/download.php?ds=pop, accessed in December 2023.

[28] Arntzen, M., "Aircraft noise calculation and synthesis in a non-standard atmosphere," Ph.D. Thesis, Delft University of Technology, Delft, the Netherlands, 2014.

[29] Rizzi, S., and Sullivan, B., "Synthesis of Virtual Environments for Aircraft Community Noise Impact Studies," *11th AIAA/CEAS Aeroacoustics Conference*, American Institute of Aeronautics and Astronautics, Monterey, California, 2005. https://doi.org/10.2514/6.2005-2983, URL https://arc.aiaa.org/doi/10.2514/6.2005-2983.

[30] Rizzi, S. A., and Christian, A., "A method for simulation of rotorcraft fly-in noise for human response studies," San Francisco, CA, 2015.

[31] Rietdijk, F., "Auralisation of airplanes considering sound propagation in a turbulent atmosphere," Ph.D. Thesis, Chalmers University of Technology, Gothenburg, Sweden, 2017. URL https://publications.lib.chalmers.se/records/fulltext/251306/251306.pdf.

[32] Pieren, R., Bütler, T., and Heutschi, K., "Auralization of Accelerating Passenger Cars Using Spectral Modeling Synthesis," *Applied Sciences*, Vol. 6, No. 5, 2016, pp. 1–27. https://doi.org/10.3390/app6010005.

[33] Åbom, M., Johansson, A., Bolin, K., and Basu, S., "Approach Noise Trials," Technical report for the KTH/Novair project Approach Noise Trials (ANT), KTH Royal Institute of Technology, Stockholm, Sweden, Apr. 2021. URL https://www.kth.se/polopoly_fs/1.1139614.1643808790!/Approach%20Noise%20Trials_Report.pdf, accessed in December 2023.

[34] Johansson, A., "Final Approach : Measurements and Ratings of Aircraft Landing Noise," Ph.D. thesis, KTH Royal Institute of Technology, Stockholm, 2023.

[35] Allen, M. P., "Analysis and Synthesis of Aircraft Engine Fan Noise for Use in Psychoacoustic Studies," Master's thesis, Virginia Polytechnic Institute and State University, Blacksburg, Virginia, Apr. 2012.

[36] Merino-Martinez, R., and Snellen, M., "Implementation of tonal cavity noise estimations in landing gear noise prediction models," *AIAA AVIATION 2020 FORUM*, American Institute of Aeronautics and Astronautics, 2020. https://doi.org/10.2514/6.2020-2578, URL https://arc.aiaa.org/doi/10.2514/6.2020-2578.

[37] Dobrzynski, W., "Almost 40 Years of Airframe Noise Research: What Did We Achieve?" *Journal of Aircraft*, Vol. 47, No. 2, 2010, pp. 353–367. https://doi.org/10.2514/1.44457, URL https://arc.aiaa.org/doi/10.2514/1.44457, publisher: American Institute of Aeronautics and Astronautics.

[38] Merino-Martinez, R., Neri, E., Snellen, M., Kennedy, J., Simons, D. G., and Bennett, G. J., "Multi–approach study of nose landing gear noise," *Journal of Aircraft*, Vol. 57, No. 3, 2020, pp. 517–533. https://doi.org/10.2514/1.C035655, URL https://doi.org/10.2514/1.C035655.

[39] Pieren, R., Bertsch, L., Lauper, D., and Schäffer, B., "Improving future low-noise aircraft technologies using experimental perception-based evaluation of synthetic flyovers," *Science of The Total Environment*, Vol. 692, 2019, pp. 68–81. https://doi.org/10.1016/j.scitotenv.2019.07.253, URL https://www.sciencedirect.com/science/article/pii/S0048969719333674.

[40] Thoma, E. M., Merino-Martínez, R., Grönstedt, T., and Zhao, X., "Noise from Flight Procedure Designed with Statistical Wind: Auralization and Psychoacoustic Evaluation," , 2024. URL https://research.chalmers.se/en/publication/540238.

[41] Merino-Martinez, R., Pieren, R., and Schäffer, B., "Holistic approach to wind turbine noise: From blade trailing–edge modifications to annoyance estimation," *Renewable and Sustainable Energy Reviews*, Vol. 148, No. 111285, 2021, pp. 1–14. https://doi.org/10.1016/j.rser.2021.111285, URL https://doi.org/10.1016/j.rser.2021.111285.

[42] Merino-Martinez, R., Pieren, R., Schäffer, B., and Simons, D. G., "Psychoacoustic model for predicting wind turbine noise annoyance," 24^{th} *International Congress on Acoustics (ICA), October 24 – 28 2022, Gyeongju, South Korea*, 2022. URL https://www.researchgate.net/publication/364996997_Psychoacoustic_model_for_predicting_wind_turbine_noise_annoyance.

[43] Greco, G. F., Merino-Martínez, R., Osses, A., and Langer, S. C., "SQAT: a MATLAB-based toolbox for quantitative sound quality analysis," *52th International Congress and Exposition on Noise Control Engineering*, Vol. 268, International Institute of Noise Control Engineering (I-INCE), Chiba, Greater Tokyo, Japan, 2023, pp. 7172–7183. https://doi.org/10.3397/IN{_}2023{_}1075.

[44] "ISO norm 532–1 – Acoustics – Method for calculating loudness – Zwicker method," Tech. Rep. 1, International Organization for Standardization, 2017. URL https://www.iso.org/obp/ui/#iso:std:iso:532:-1:ed-1:v2:en.

[45] Aures, W., "Procedure for calculating the sensory euphony of arbitrary sound signal. In German: Berechnungsverfahren für den sensorischen Wohlklang beliebiger Schallsignale," *Acustica*, Vol. 59, No. 2, 1985, pp. 130–141. URL https://www.ingentaconnect.com/contentone/dav/aaua/1985/00000059/00000002/art00008.

[46] von Bismark, G., "Sharpness as an attribute of the timbre of steady sounds," *Acta Acustica united with Acustica*, Vol. 30, No. 3, 1974, pp. 159–172. URL https://www.semanticscholar.org/paper/Sharpness-as-an-attribute-of-the-timbre-of-steady-Bismarck/9576a2a74bff46ee0cded25bfd9e4302b4fb0470.

[47] Daniel, P., and Webber, R., "Psychoacoustical Roughness: Implementation of an Optimized Model," *Accustica – acta acustica*, Vol. 83, 1997, pp. 113–123. URL https://www.ingentaconnect.com/contentone/dav/aaua/1997/00000083/00000001/art00020.

[48] Osses, A., García León, R., and Kohlrausch, A., "Modelling the sensation of fluctuation strength," 22^{nd} *International Congress on Acoustics (ICA), September 5 – 9 2016, Buenos Aires, Argentina*, 2016. URL https://pure.tue.nl/ws/portalfiles/portal/52366479/Osses_Garcia_Kohlrausch_ICA2016_ID113.pdf.

[49] Di, G.-Q., Chen, X.-W., Song, K., Zhou, B., and Pei, C.-M., "Improvement of Zwicker's psychoacoustic annoyance model aiming at tonal noises," *Applied Acoustics*, Vol. 105, 2016, pp. 164–170. https://doi.org/10.1016/j.apacoust.2015.12.006, URL http://dx.doi.org/10.1016/j.apacoust.2015.12.006.

[50] Greco, G. F. and Merino-Martinez, R. and Osses, A., "SQAT: a sound quality analysis toolbox for MATLAB (version v1.0)," , May 2023. URL https://zenodo.org/records/7934710#.ZGD-H3ZBxhF, accessed in May 2023.

[51] Greco, G. F. and Merino-Martinez, R. and Osses, A., "SQAT: a sound quality analysis toolbox for MATLAB," , May 2023. URL https://github.com/ggrecow/sqat, accessed in May 2023.